Design and Implementation of a Capacitive-Type Microphone With Rigid Diaphragm and Flexible Spring Using the Two Poly Silicon Micromachining Processes

Chun-Kai Chan, Wei-Cheng Lai, Mingching Wu, Ming-Yung Wang, and Weileun Fang

***Abstract*—This study reports the design and implementation of a novel capacitive-type micromachined microphone. The design of the microphone is based on the well-known two poly-Si layers micromachining processes. The microphone consists of a rigid diaphragm (the 2nd poly-Si layer), flexible springs (the 1st ply-Si layer), and rigid back plate (the 1st poly-Si layer). In short, the proposed microphone design has four merits, (1) the rigid diaphragm acting as the acoustic wave receiver and moving electrode is realized using the rib-reinforced poly-Si layer, (2) the flexible spring acting as the electrical routing as well as supporter for diaphragm is implemented using the thin poly-Si film, (3) the electrical routing of rigid diaphragm (moving electrode) is through the central poly-via and the flexible spring, and (4) the rigid plate acting as the stationary electrodes and back plate is fabricated using the high-aspect-ratio (HARM) trench-refilled poly-Si. To demonstrate the feasibility, the two poly-Si microphone has been implemented and tested. Typical measurement results show that the open-circuit sensitivity of the microphone was 12.63 mV/Pa (−37.97 dBV/Pa) at 1 kHz. (the reference sound-level is 94 dB).**

***Index Terms*—Acoustic transducers, capacitive sensor, MEMS microphone, , poly-via, rib-reinforced, rigid diaphragm, silicon condenser microphone.**

I. Introduction

MICROPHONES converting acoustic input to electrical output are very popular devices in the multimedia applications such as mobile phone, computer, hearing aid, and consuming products. Most of the traditional Electret Condenser Microphones (ECMs) are assembled by polymer diaphragms, thus the surface mount process with soldering reflow temperature higher than 260°C is a critical concern. Recently, the MEMS microphones made by semiconductor processes are emerging to replace the ECM microphones because of compact size, high signal-to-noise ratio, high sensitivity, quick response, and long-term stability [1]. In addition, the diaphragms made by single crystal Si or polycrystalline Si provide great temperature stability and are compatible with soldering reflow process. In short, the MEMS technology is considered as a promising approach to implement microphones.

Presently, various structure designs and micromachining processes for MEMS microphones have been extensively reported [2]–[13]. The well-known surface micromachining process consisted of two poly-Si structure layers has successfully been employed to realize a commercial microphone [7]. The existing capacitive microphones typically consist of a flexible diaphragm and a rigid back plate separated by air gap. The flatness of flexible diaphragm plays an important role for the performance of MEMS microphone [14]. However, the flatness of micromachined structure is frequently influenced by the residual stresses of thin film induced during the fabrication processes [15], [16]. Unfortunately, it is not straightforward to control the residual stresses of thin film during the processes. Thus, various MEMS microphone designs have been investigated to reduce the influence of thin film residual stresses [17]–[19]. For instance, the diaphragm anchored on the cantilever beam is developed [7], so that the residual stress was released from the free end. The corrugation ring around the diaphragm is employed to release the residual stress in [20], [21]. In addition, to fabricate the diaphragm using the device Si layer of SOI (Si on insulator) wafer also provides a solution prevent the residual stress problem for MEMS microphone [22].

Instead of flexible diaphragm, this study proposed a microphone consisted of a rigid diaphragm supported by flexible springs. Thus, the deformation of diaphragm by thin film residual stress can be significantly reduced. In addition, the poly-Si flexible spring is employed to support the rigid diaphragm by central poly-Si via and provide a sensitive mechanism to convert sound pressure into capacitance change. Therefore, the rigid diaphragm anchored on the flexible spring is allowed to oscillate after subjected with the sound pressure. The sound pressure is then detected by the capacitance change between the movable diaphragm and the stationary back plate. To demonstrate

Manuscript received January 30, 2011; revised February 16, 2011; accepted February 16, 2011. Date of publication February 28, 2011; date of current version August 12, 2011. This work was supported in part by the National Science Council of Taiwan under Grant NSC 96-2628-E-007-008. The associate editor coordinating the review of this manuscript and approving it for publication was Prof. Boris Stoeber.

C.-K. Chan is with Power Mechanical Engineering Department, National Tsing Hua University, Hsinchu 30013, Taiwan (e-mail: d9533810@oz.nthu.edu.tw).

W.-C. Lai is with Institute of NanoEngineering and MicroSystems, National Tsing Hua University, Taiwan (e-mail: sonic33228@gmail.com).

M. Wu is with Domintech Co. Ltd., Taipei County 248, Taiwan (e-mail: ericw@domintech.com.tw).

M.-Y. Wang is with Tatung University, Taipei City 104, Taiwan (e-mail: mywang@ttu.edu.tw).

W. Fang is with Power Mechanical Engineering Department, National Tsing Hua University, Hsinchu 30013, Taiwan, and also with Institute of NanoEngineering and MicroSystems, National Tsing Hua University, Hsinchu 30013, Taiwan (e-mail: fang@pme.nthu.edu.tw).

Color versions of one or more of the figures in this paper are available online at http://ieeexplore.ieee.org.

Digital Object Identifier 10.1109/JSEN.2011.2121060

1530-437X/$26.00 © 2011 IEEE

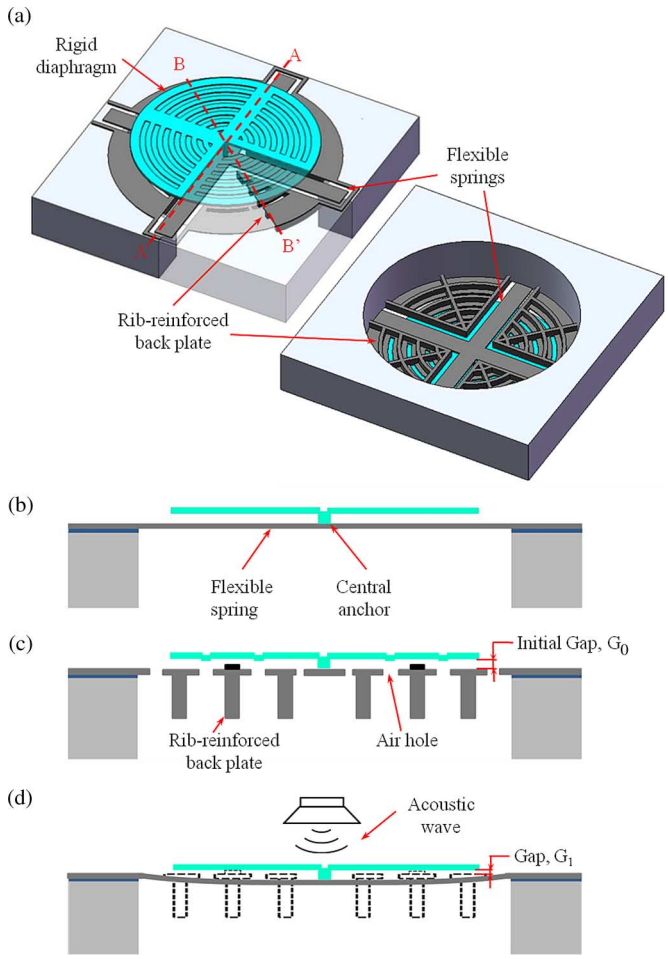

Fig. 1. Schematic illustrations of the proposed microphone design, (a) isometric views respectively from front-side and backside, (b) the AA' cross section view, (c) the BB' cross section view, and (d) the capacitance change of the microphone resulted from the motion of the rigid diaphragm and the deflection of the flexible springs.

the feasibility of the design, this study also employs the two poly-Si MOSBE II processes [23] to implement the proposed microphone.

II. Concepts and Design

This study presents a capacitive sensing microphone design, and further employs the two poly-Si MOSBE II process [23] to implement the device using the two poly-Si layers on Si substrate. Fig. 1 illustrates the design of the proposed microphone. Fig. 1(a) schematically shows the top-side and backside views of the microphone on the Si substrate. As indicated in the top-side view illustration, the microphone consists of a rigid diaphragm (the 2nd poly-Si layer), flexible springs (the 1st poly-Si layer), and rigid back plate (the 1st poly-Si layer). The backside view illustration shows an opening on the Si substrate. Fig. 1(b), (c) further illustrate the cross sections of AA' and BB' depicted in Fig. 1(a). The AA' cross section view shows the rigid diaphragm is anchored to the flexible spring, and the flexible spring is fixed to the Si substrate. The BB' cross section view shows the rigid back plate fixed to the Si substrate, and the initial sensing gap G_0 between the rigid diaphragm and the back plate. Moreover,

TABLE I
Detail Information of the Microphone Design

DESIGN CONDITIONS	
Diaphragm radius	500 μm
Diaphragm thickness	3 μm
Air gap length	2 μm
Spring thickness	2 μm
Spring dimensions	600 μm×30 μm
Dimple thickness	0.5 μm
Resonant frequency	24.9 kHz

the air holes are designed on the rigid plate. This study further employs the anchor and the springs as the electrical routing for the rigid diaphragm (movable electrode). As shown in Fig. 1(d), the flexible spring will be deformed when the sound pressure applying on the rigid diaphragm. The dynamic response of the spring-diaphragm system is occurred. Thus, the gap between the rigid diaphragm (movable electrode) and the back plate (stationary electrode) is changed from G_0 to G_1; and further lead to a capacitance change ΔC. Finally, the microphone converts the acoustic signals to electrical signals according to the ΔC. In short, the proposed microphone design in Fig. 1 has four merits, (1) the rigid diaphragm acting as the acoustic wave receiver and moving electrode is realized using the rib-reinforced poly-Si layer [24]–[28], (2) the flexible spring acting as the electrical routing as well as supporter for diaphragm is implemented using the thin poly-Si film, (3) the electrical routing of rigid diaphragm (moving electrode) is through the central poly-via and the flexible spring, and (4) the rigid plate acting as the stationary electrodes and back plate is fabricated using the high-aspect-ratio (HARM) trench-refilled poly-Si.

This study has employed the commercial finite element software (ANSYS) to evaluate the characteristics of the proposed design. Table I summarizes the dimensions of a typical microphone design. By means of the finite element analysis, the natural frequencies and vibration modes of the spring-diaphragm structure are predicted. Fig. 2(a) shows the model established for the finite element analysis. The typical result from finite element analysis in Fig. 2(b) shows the first resonant frequency of the spring-diaphragm structure is 24.9 kHz. Thus, the microphone could be employed to detect sound between 20 Hz and 20 kHz. According to the modal analysis, the diaphragm acts as a rigid body and has only up-down linear oscillation in the out-of-plane direction (Y-axis) for the first vibration mode. In the mean time, the springs experience the transverse bending deformation in the out-of-plane direction. As discussed in Fig. 1(d), such linear out-of-plane oscillation of the diaphragm will lead to the variation of sensing gap and the capacitance of the microphone. Moreover, the spring-diaphragm structure has a repeated resonant frequency of 28.1 kHz for the vibration modes respectively shown in Fig. 2(c), (d). The vibration modes are the angular oscillations of rigid diaphragm respectively about the X-axis and Z-axis. Thus, any combination of these two vibration modes could occur at the natural frequency of 28.1 kHz.

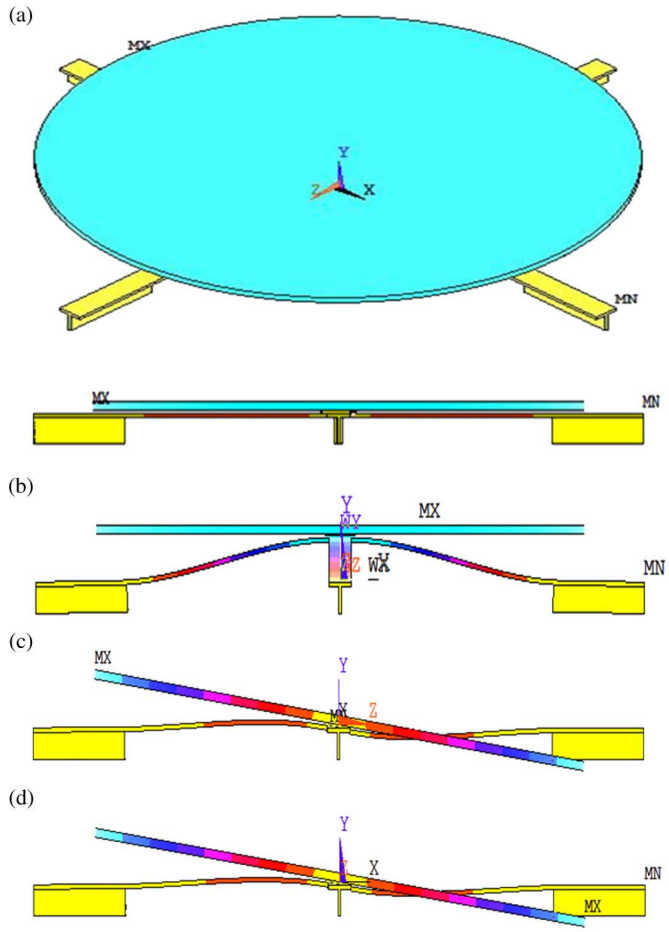

Fig. 2. Typical finite element simulation model and results. (a) Simulation model. (b) 1st mode: out-of-plane linear oscillation of the diaphragm. (c) 2nd mode: angular oscillation of the diaphragm about the X-axis. (d) 3rd mode: angular oscillation of the diaphragm about the Z-axis.

III. Fabrication and Results

To demonstrate the feasibility of the proposed design in Fig. 1, this study has established the fabrication process to implement the microphone based on the double poly-Si MOSBE II process in [23]. Fig. 3 illustrates the process steps to realize the proposed microphone. The processes began with the growth of thermal oxide on a Si wafer, and then the oxide was patterned to define the in-plane shape of rib-reinforced back plate. After that, the DRIE (deep reactive ion etching) was employed to etch trenches on the Si substrate, as shown in Fig. 3(a). The depth of trenches defines the thickness of ribs on the rein-forced rigid back plate. As shown in Fig. 3(b), the 1st sacrificial oxide layer was thermally grown on the Si substrate. This thermal oxide was also acted as the protection layer for the following backside DRIE Si etching. After that, the 1st poly-Si layer (Poly1) was deposited using the LPCVD (low pressure chemical vapor deposition), and the trench was thus refilled by Poly1. Thus, the flexible spring was formed by the thin Poly1; meanwhile the stiff back plate was realized by the trench-refilled thick Poly1. As illustrated in Fig. 3(c), the Poly1 on substrate surface was patterned by RIE, and then LPCVD nitride was deposited and patterned as dimple. The dimple structure is employed to avoid the short circuit between the movable electrode and stationary

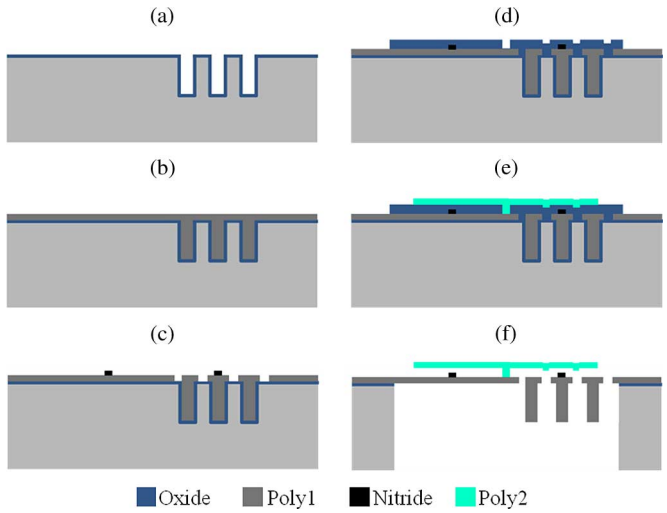

Fig. 3. Fabrication process steps. (a) Etch-trench. (b) Trench-refill. (c) Dimple. (d) Sacrifice layer. (e) Rigid membrane. (f) Backside etching.

electrode during the contact of diaphragm and back plate. After that, the PECVD (plasma enhanced chemical vapor deposition) oxide was deposited and patterned as the 2nd sacrifice layer to define the sensing gap, as shown in Fig. 3(d). The 2nd poly-Si layer (Poly2) was then deposited and patterned to define the rib-reinforced rigid diaphragm, as shown in Fig. 3(e). As shown in Fig. 3(f), the backside DRIE was employed to remove Si substrate underneath the microphone. During the backside DRIE, the 1st sacrificial oxide acted as the etching stop layer. Finally, the protection and the sacrificial oxide layers were removed using the HF solution to fully release the microphone from the Si substrate.

The SEM (scanning electron microscopy) micrographs in Fig. 4 show the typical fabrication results of the proposed microphone. Fig. 4(a) and 4(b) respectively show the front-side view and backside view of the microphone. The circular diaphragm and the back plate are respectively demonstrated in the front-side view and backside view micrographs. As indicated in Fig. 4(b), the rigid back plate is fixed to the Si substrate. The Si substrate patterned by the backside DRIE is demonstrated in the micrograph. Moreover, the grid patterns in the micrograph indicate the back plate with reinforced rib underneath. As indicated in Fig. 4, the diaphragm is made of the Poly2 layer, and the back plate with HARM ribs is made of the Poly1 layer. The SEM micrographs in Fig. 4(c)–(h) show more detail fabrication results of the microphone. The micrograph in Fig. 4(c) shows the rib-reinforced structures distributed on the diaphragm, hence the stiffness of diaphragm is increased. The zoom-in micrograph in Fig. 4(d), (e) shows the center of diaphragm anchored to the springs underneath. This central anchor also acts as the electrical routing for the movable electrode on diaphragm. Fig. 4(e) also shows the gap defined by the 2nd sacrificial oxide layer to provide a vertical moving space between the diaphragm and back plate. After removing the rigid diaphragm, the flexible spring underneath is observed, as the SEM micrograph shown in Fig. 4(f). The etching hole at the backside of the Si substrate is also observed. The zoom-in micrograph in Fig. 4(g) shows the back side view

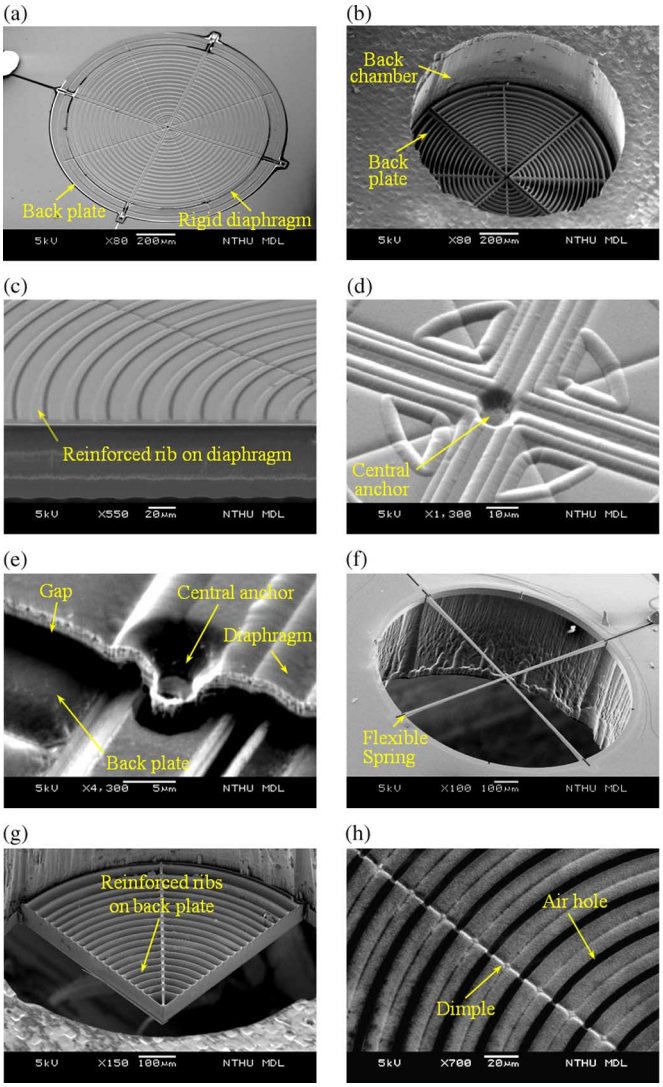

Fig. 4. SEM micrographs of typical fabricated microphone. (a) Front-side view. (b) Backside view. (c) Cross section of the rib-reinforced rigid diaphragm. (d)–(e) Zoom-in of the central anchor of the diaphragm. (f) Flexible spring after the removing of the diaphragm. (g) Backside view of the back plate with HARM reinforced ribs. (h) Front-side view of the back plate with air holes and dimples.

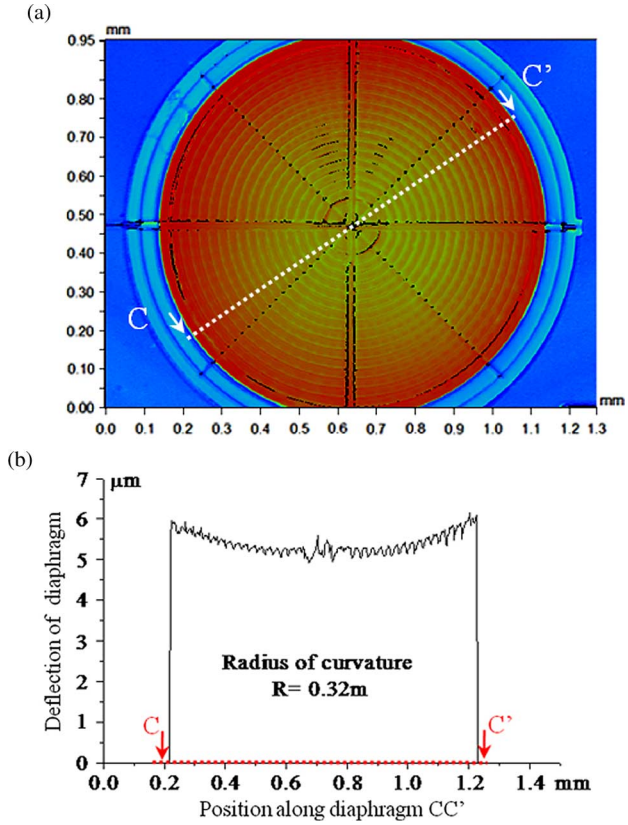

Fig. 5. Surface profile of rigid diaphragm measured by the optical interferometer. (a) Top view. (b) Surface profile of diaphragm along the cross section CC′.

of the substrate, and thus the back plate is clearly observed. The HARM ribs to significantly increase the stiffness of the back plate are demonstrated. The depth of reinforced rib is defined by the DRIE trenches, and these trenches are then refilled by the Poly1 layer. The zoom-in micrograph in Fig. 4(h) further shows the front-side view of the back plate. The air hole and the dimple are precisely aligned on back-plate using the process.

IV. Measurement

This study has performed various tests to characterize the static and dynamic characteristics of the fabricated microphone. Firstly, the initial deformation of the diaphragm was characterized using the commercial optical interferometer. The measurement results in Fig. 5(a) show the top view of the diaphragm. The colors indicate the surface profile of the diaphragm. The measurement results in Fig. 5(b) show the deformation profile of the diaphragm along the CC′ cross section depicted in Fig. 5(a). The ripples are resulted from the rib-reinforced ribs. The measurement shows the diaphragm has a radius of curvature of 0.32 m. It demonstrates the superior diaphragm flatness achieved by the proposed rib-reinforced structure design. The initial deformation of diaphragm resulted from the residual stress of Poly2 layer is reduced. Secondly, the dynamic response of the microphone was characterized using the commercial Laser Doppler Vibrometer (LDV). In this test, the mechanical structure of the microphone was excited using the piezoelectric transducers. The measurement results show that the typical 1st resonant frequency of the microphone is 26 kHz.

After that, the microphone was wire bonded and packaged on a metal can as the DUT (device under test) for functional tests. The photo in Fig. 6(a) shows the DUT, and the zoom-in photo in Fig. 6(b) shows the diaphragm, bond pads, and wires. The microphone device was bonded on a circular metal can (1 cm in diameter) with anaerobic adhesive. The measurement setup in Fig. 7 was established to characterize the performance of the microphone. The microphone was placed inside a semi-anechoic chamber for test. The semi-anechoic chamber is a laboratory space with special wall, but not floor, to minimize the external noise and sound reflections. During the test, the loudspeaker (TANNOY) was used to specify a sound pressure to excite the microphone, and the sound pressure level monitored by a commercial sound-level meter (B&K-2230). The DUT was electrical connected to the commercial capacitance readout IC (MS3110).

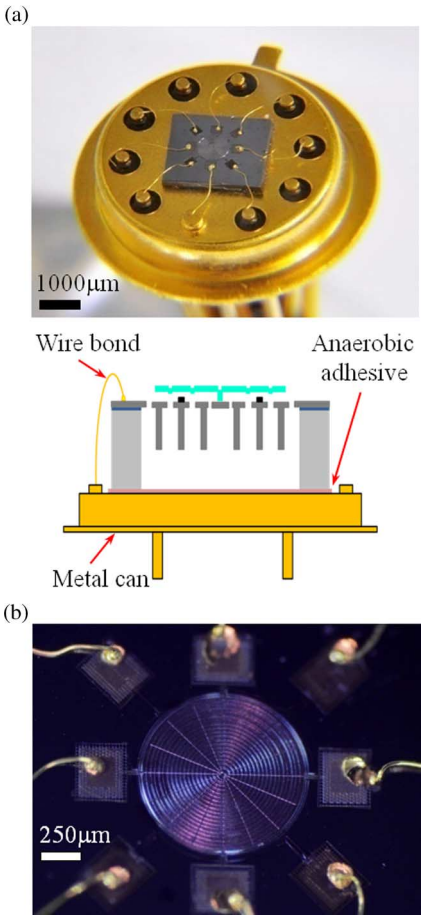

Fig. 6. (a) Fabricated microphone after bonded and packaged on a metal can. (b) Zoom-in photo to show the diaphragm, bond pads, and wires.

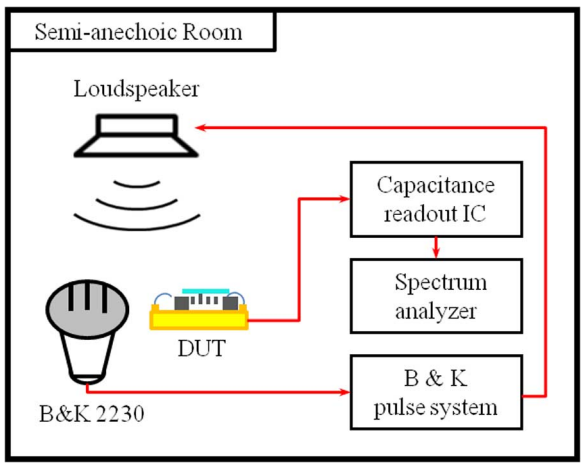

Fig. 7. Experiment setup for the acoustic performance measurement of microphone.

Thus, the output signals from the capacitance readout IC were recorded by the spectrum meter. Fig. 8 shows the typical measured results. As shown in Fig. 8(a), the open-circuit sensitivity of the microphone was 12.63 mV/Pa (−37.97 dBV/Pa) at 1 kHz. The reference sound level was 94 dB. The measured and predicted initial capacitances are respectively 2.60 pF, and 1.81 pF. Thus, the parasitic capacitance which mainly induced from the

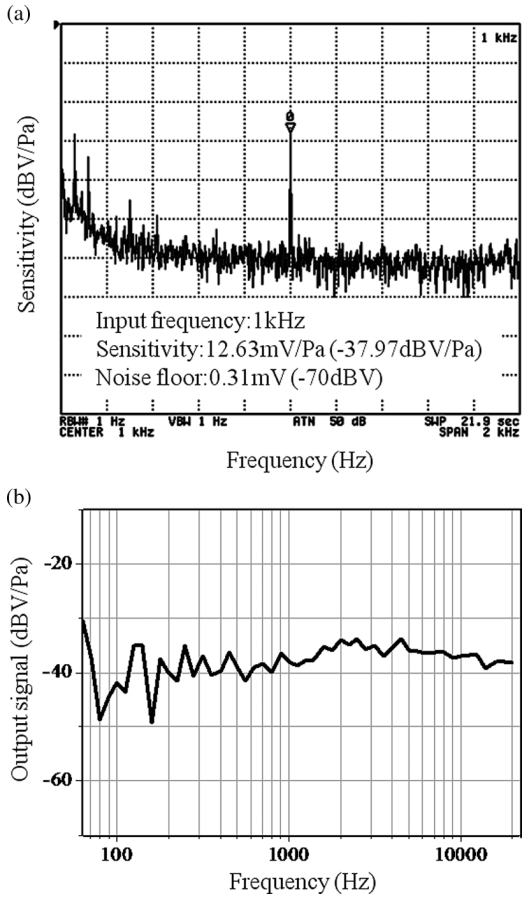

Fig. 8. Typical measurement results of the fabricated microphone. (a) Open-circuit sensitivity. (b) Frequency response.

TABLE II
THE TYPICAL MEASUREMENT RESULTS OF THE FABRICATED MICROPHONE

MEASUREMENT RESULT	
Resonant frequency	26 kHz
Input signal bandwidth	60Hz-20 kHz
Initial capacitance	1.81 pF
Circuit gain	2 V/V
Sensitivity (1kHz)	-37.97 dBV/Pa
Output voltage (1kHz)	12.63 mV/Pa
Noise floor	0.31 mV(-70 dBV)

diaphragm and backplate is estimated as 0.79 pF. The measurement results in Fig. 8(b) show the frequency response of microphone. The input signal bandwidth ranges from 60 Hz to 20 kHz. Moreover, as shown in Fig. 1(c), the diaphragm of the presented microphone has an initial gap G_0 with the backplate. Thus, such surrounding opening of the diaphragm will cause leakage of the acoustic pressure, and further lead to the uneven frequency response at lower frequency range [29]. Measurement results in Table II summarize the characteristics of a typical fabricated microphone. The comparison results of the existing microphones and this work in Table III.

TABLE III
COMPARISON OF THE EXISTING MICROPHONES AND THIS WORK

	P. V. Loeppert [7]	M. Goto[8]	B. A. Ganjia [11]	This study
Diaphragm size	Diameter: 0.56mm	Diameter: 2mm×2mm	Square: 0.5mm×0.5mm	Diameter: 1mm
Diaphragm thickness	1μm	4μm	3μm	3μm
Air gap	4μm	10μm	1μm	2μm
Bias voltage	11V	48V	105V	-
Sensitivity	7.94mV/Pa	6.683mV/Pa	0.2mV/Pa	12.63 mV/Pa

V. CONCLUSIONS

This study presents the design of a microphone consisting of a rigid diaphragm, flexible springs, and rigid HARM back plate. The rigid diaphragm is anchored to the flexible springs by means of a central via, and the sound pressure will be detected by the dynamic response of the spring-diaphragm structure. The microphone is successfully fabricated using an existing two poly-Si MOSBE II micromachining processes. The process technologies such as DRIE and trench refilled poly-Si have been employed to implement the HARM thin film structures. The initial deformation of diaphragm due to the thin film residual stresses is significantly reduced. Moreover, the tests demonstrate the performances such as sensitivity and frequency range of the device. The flat frequency response of the microphone is from 200 Hz to 20 kHz. The open-circuit sensitivity of the microphone is 12.63 mV/Pa (−37.97 dBV/Pa) at 1 kHz. (reference sound-level is 94 dB). The noise floor is 0.31 mV (−70 dBV). However, the sensitivity of the proposed microphone design at low frequency range still needs to be further improved. Moreover, despite the reasonable sensitivity of presented microphone, the device under test (consisting of Microphone chip, the capacitance readout IC on printed circuit board, and their electrical interconnection) has large noise. The primary reason leads to the large noise is the relatively long electric wires required for the connection of MEMS chip and the packaged capacitance readout IC. The length of electrical interconnection can be significantly reduced as the MEMS chip can be directly bonded with the chip of capacitance readout IC. Thus, the noise can be significantly decreased. Moreover, the fluctuation of frequency response (±3.5 dB) from 200 Hz to 20 kHz can also be improved.

ACKNOWLEDGMENT

The authors wish to thank the National Tsing Hua University, National Chiao Tung University, National Taiwan University, and the NDL (National Nano Device Laboratory) of National Science Council for providing the fabrication facilities.

REFERENCES

[1] G. M. Sessler, "Silicon microphones," *J. Audio Eng. Soc.* , vol. 44, pp. 16–21, 1996.
[2] W. Kuhnel, "Silicon condenser microphone with integrated field effect transistor," *Sens. Actuat. A*, vol. 25–27, pp. 521–525, 1991.
[3] T. Bourouina, S. Spirkovitch, F. Baillieu, and C. Vauge, "A new condenser microphone with a P + silicon membrane," *Sens. Actuat. A*, vol. 31, pp. 149–152, 1992.
[4] E. Graf, W. Kronast, S. Diihring, B Muller, and A. Stoffel, "Silicon membrane condenser microphone with integrated field-effect transistor," *Sens. Actuat. A*, vol. 37–38, pp. 708–711, 1993.
[5] X. Li, R. Lin, H. Kek, J. Miao, and Q. Zou, "Sensitivity-improved condenser microphone with a novel single deeply corrugated diaphragm," *Sens. Actuat. A*, vol. 92, pp. 257–262, 2001.
[6] J. J. Neumann, Jr. and K. J. Gabriel, "CMOS-MEMS membrane for audio-frequency acoustic actuation," *Sens. Actuat. A*, vol. 95, pp. 175–182, 2002.
[7] P. V. Loeppert and S. B. Lee, "SiSonicTM—The first commercialized MEMS microphone," in *Proc. Solid-State Sensors, Actuators, and Microsystems Workshop*, Hilton Head Island, SC, Jun. 2006, pp. 27–30.
[8] M. Goto, Y. Iguchi, K. Ono, A. Ando, F. Takeshi, S. Matsunaga, Y. Yasuno, K. Tanioka, and T. Tajima, "High-performance condenser microphone with single-crystalline silicon diaphragm and backplate," *IEEE Sens. J.*, vol. 7, pp. 4–10, 2007.
[9] Z.-Z. Shu, M.-L. Ke, G.-W. Chen, R.-H. Homg, C.-C. Chang, J.-Y. Tsai, C.-C. Lai, and J.-L. Chen, "Design and fabrication of condenser microphone using wafer transfer and micro-electroplating technique," in *Proc. Dans Symp. Design, Test, Integration and Packaging of MEMS/MOEMS*, Nice, France, May 2008, pp. 386–390.
[10] S. S. Je, J. Kim, J. C. Harrison, M. N. Kozicki, and J. Chae, "In-situ tuning of omnidirectional micro-electro-mechanical-systems microphones to improve performance fit in hearing aids," *Appl. Phys. Lett.*, vol. 93, pp. 12350-1–12350-3, 2008.
[11] B. A. Ganjia and B. Y. Majlis, "Design and fabrication of a new MEMS capacitive microphone using a perforated aluminum diaphragm," *Sens. Actuat. A*, vol. 149, pp. 29–37, 2009.
[12] J. Citakovic, F. Hovesten, G. Rocca, A. Van Halteren, P. Rombach, L. Stenberg, P. Andreani, and E. Bruun, "A compact CMOS MEMS microphone with 66 dB SNR," in *Proc. IEEE Int. Solid-State Circuits Conf.*, San Francisco, CA, Feb. 2009, pp. 350–351.
[13] J. Krause and R. D. White, "MEMS microphone array on a chip," *J. Acoust. Soc. Amer.*, vol. 127, p. 1980, 2010.
[14] B. Cunningham and J. Bernstein, "Wide bandwidth silicon nitride membrane microphones," in *Proc. SPIE Micromach. Microfab. Process Technology III*, 1997, vol. 3223, pp. 56–63.
[15] H. Guckel, T. Randazzo, and D. W. Burns, "A simple technique for the determination of mechanical strain in thin films with application to polysilicon," *J. Appl. Phys.*, vol. 57, pp. 1671–1675, 1985.
[16] H. Guckel, D. W. Burns, C. C. G. Visser, H. A. C. Tilmans, and D. Deroo, "Fine-grained polysilicon films with built-in tensile strain," *IEEE Trans. Electron. Devices*, vol. 35, no. 6, pp. 800–801, Jun. 1988.
[17] H. Guckel, J. J. Sniegowski, and T. R. Christenson, "Fabrication of micromechanical devices from polysilicon films with smooth surfaces," *Sens. Actuat. A*, vol. 20, pp. 117–122, 1989.
[18] X. Zhang, T.-Y. Zhang, M. Wong, and Y. Zohar, "Residual-stress relaxation in polysilicon thin films by high-temperature rapid thermal annealing," *Sens. Actuat. A*, vol. 64, pp. 109–115, 1998.
[19] J. Yang, H. Kahn, A.-Q. He, S. M. Phillips, S. Member, and A. H. Heuer, "A new technique for producing large-area as-deposited zero-stress LPCVD polysilicon films: The multiPoly process," *IEEE J. Microelectromech. Syst.*, vol. 9, no. 4, pp. 485–494, Dec. 2000.
[20] P. R. Scheeper, W. Olthuis, and P. Bergveld, "The design, fabrication and testing of corrugated silicon nitride diaphragms," *IEEE J. Microelectromech. Syst.*, vol. 3, no. 1, pp. 36–42, Mar. 1994.

[21] J. Miao, R. Lin, L. Chen, Q. Zou, S. Y. Lim, and S. H. Seah, "Design considerations in micromachined silicon microphones," *Microelectron. J.*, vol. 33, pp. 21–28, 2002.
[22] J. W. Weigold, T. J. Brosnihan, J. Bergeron, and X. Zhang, "A MEMS condenser microphone for consumer applications," in *Proc. IEEE MEMS*, Istanbul, Turkey, 2006, vol. 22–26, pp. 86–89.
[23] M. Wu and W. Fang, "The molded surface-micromachining and bulk etching release (MOSBE) fabrication platform on (111) Si for MOEMS," *J. Micromech. Microeng.*, vol. 16, pp. 260–265, 2005.
[24] C. G. Keller and R. T. Howe, "HEXSIL tweezers for teleoperated micro-assembly," in *Proc. IEEE MEMS'97*, Nagoya, Japan, June 1997, pp. 72–77.
[25] E. K. Demirlioglu, "Trench Refill With Selective Polycrystalline Materials," U.S. Patent 5 994 718, 1999.
[26] H.-Y. Lin and W. Fang, "Rib-reinforced micromachined beam and it applications," *J. Micromech. Microeng.*, vol. 10, pp. 93–99, 2000.
[27] J. Chae, H. Kulah, and K. Najafi, "A monolithic three axis micro-g micromachined silicon capacitive accelerometer," *IEEE J. Microelectromech. Syst.*, vol. 14, no. 2, pp. 235–242, Apr. 2005.
[28] M. Wu and W. Fang, "Design and fabrication of MEMS devices using the integration of MUMPs, trench-refilled molding, DRIE, and bulk silicon etching processes," *IEEE J. Microelectromech. Syst.*, vol. 15, pp. 535–542, 2005.
[29] H. S. Kwon and K. C. Lee, "Double-chip condenser microphone for rigid backplate using DRIE and wafer bonding technology," *Sens. Actuat. A*, vol. 138, pp. 81–86, 2007.

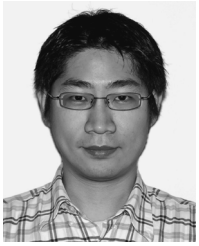

Chun-Kai Chan was born in Chiayi, Taiwan, in 1977. He received the M.S. degree from the Institute of Mechanical Engineering at Tatung University, Taipei City, Taiwan, in 2006. He is currently pursuing the Ph.D. degree in power mechanical engineering, National Tsing Hua University, Taiwan.

His major research interests include Si based micromachining process, MEMS capacitive sensors (accelerometer, microphone) and sensors integration.

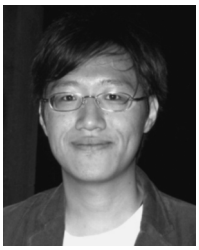

Wei-Cheng Lai was born in Taipei, Taiwan, in 1986. He received the M.S. degree from the Institute of NanoEngineering and MicroSystems at National Tsing Hua University, Taiwan, in 2010.

His major research interests include MEMS fabrication process, and MEMS application in Neuroscience research.

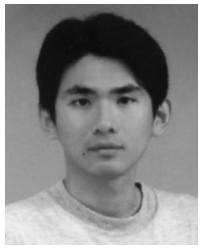

Mingching Wu was born in Taoyuan, Taiwan. He received the Ph.D. degree in power mechanical engineering (PME) in 2005 from the National Tsing-Hua University, Taiwan.

He has been working in the MEMS field for 10 years and his research interests include Si based micromachining process, MEMS sensors, and optical scanning mirror. In 2006, he jointed the R&D division in ChipSense, Taiwan, and developed the 3-axis accelerometer. In 2009, the product is successfully commercialized and to be the first and solely 3-axis MEMS accelerometer in Taiwan. He is working for Domintech and intends to develop more functionality MEMS sensors now.

Ming-Yung Wang was born in Taiwan.

He has been working in the field of mechanical engineering for 40 years. He joined the Department of Mechanical Engineering at the Tatung University in 1968. His major research interests include computer aided design, and solid mechanics.

Weileun Fang was born in Taipei, Taiwan. He received the Ph.D. degree from Carnegie Mellon University, Pittsburgh, PA, in 1995. His doctoral research focused on the determining of the mechanical properties of thin films using micromachined structures.

In 1995, he worked as a postdoctoral research at Synchrotron Radiation Research Center, Taiwan. He joined the Power Mechanical Engineering Department at the National Tsing Hua University, Taiwan, in 1996, where he is now a Professor as well as a faculty of NEMS Institute. In 1999, he was with Prof. Y.-C. Tai at California Institute of Technology, Pasadena, as a Visiting Associate. His research interests include MEMS with emphasis on micro fabrication/packaging technologies, CMOS MEMS, CNT MEMS, micro optical systems, micro sensors and actuators, and characterization of thin film mechanical properties. He has published more than 100 SCI journal papers, near 200 international conference papers, and 60 patents (all in MEMS field).

Prof. Fang is the a Board Member of JMM, and the Associate Editor of IEEE SENSORS JOURNAL, and JM3. He has served as the Chief Delegate of Taiwan for World Micromachine Summit since 2008. He also served as the TPC of IEEE MEMS conference, the EPC of Transducers conference, and the regional co-chair of IEEE Sensors conference. He has become the member of international steering committee of Transducers from 2009. Moreover, he also serves as a technical consultant for many MEMS companies in Taiwan.